Outstanding issues related to thermospheric measurements and modeling

Kenneth Moe [a], Mildred M. Moe [a] and Eelco Doornbos [b]
[a] *Space Environment Technologies, USA, kmmoe@att.net*
[b] *Aerospace Engineering, Delft University of Technology, Kluyverweg 1, 2629 HS Delft, The Netherlands, e.n.doornbos@tudelft.nl*

Abstract

Semi-empirical thermospheric models are created using measurements made in orbit. In this paper, outstanding issues regarding the interpretation of those measurements and the effects on models are considered. These include the present state of knowledge of drag coefficients, long-term trends, instrument calibration, radiation pressure, spacecraft geometry, and modeling difficulties at the 2008 solar minimum. Many recent and ongoing efforts to evaluate and improve thermospheric models are described.

1. Introduction

Models of the thermosphere are constructed from a set of differential equations that express the physical laws governing the atmosphere. The parameters in these models must be determined from measurements made in space, either directly by instruments placed in orbit, or indirectly by tracking observations of satellites undergoing orbital decay. There are outstanding issues related to the interpretation and application of these measurements. This paper is devoted to these fundamental issues.

Table 1 summarizes the uncertainties of various classes of thermospheric measurements, based on the conclusions of both the experimenters and those analyzing the space-based data. During geomagnetic storms, high thermospheric wind components along and perpendicular to the orbit track add to the uncertainties**.** Thus Table 1 refers to measurement accuracies at geomagnetically quiet times and moderately disturbed times ($5 < A_p < 25$). The uncertainties indicated for the various kinds of measurements largely represent biases, rather than statistical errors. Biases are particularly addressed by calibration of instruments and density data sets. The calibration of instruments is often a difficult task because laboratory environments are very different from the space environment. Measurements made by accelerometers and analyses of orbital decay have an advantage in accuracy, because the drag coefficients (C_d) required for their interpretation can be determined within a narrow range for a satellite of known shape, orientation, and mass. Measurements of density via satellite drag have been used in the construction of many of the semi-empirical thermospheric models that are widely used in satellite operations.

2. Drag Coefficients

It is important at the outset to distinguish clearly the two ways in which drag coefficients can be quoted. The first is the basic definition: the physical drag coefficient is determined by the momentum transfer to the satellite by the atmospheric molecules which strike and then are reemitted from the satellite surface. However, sometimes drag coefficients are approximated by fitting an atmospheric model to the observed orbital decay. Those should properly be called fitted drag coefficients. Such drag coefficients are useful in tracking and orbit determination of a specific satellite. However, any limitations of the assumed atmospheric model are then included in the derived density values. Unless

stated otherwise, throughout this work, the term drag coefficient will mean the physical drag coefficient.

The drag coefficient is a major source of uncertainty in atmospheric density measurements and models. The density ρ is often deduced from the observed drag force F_d on a satellite. The scalar form of that well-known relation is:

$$F_d = ½ \rho C_d A V_i^2 \qquad (1)$$

This equation also defines the drag coefficient, C_d. Here V_i is the speed of the incident air stream relative to the satellite. The area, A, is usually taken to be the projected area of the spacecraft normal to the velocity vector. V_i is known to high accuracy, except at high latitudes, and especially during geomagnetic storms, when large in-track winds cause uncertainties in V_i. If A is known, then C_d is the principal cause of uncertainty in calculating densities from the drag force, at altitudes below 400 km at sunspot minimum, and below 600 km at sunspot maximum. Above these altitudes, solar radiation pressure can become the major cause of error (see Section 7).

The drag coefficient depends on the satellite shape and orientation. It also depends on the way in which incident molecules interact with the satellite surfaces. Laboratory experimenters have been measuring the interaction of molecules with surfaces for the past century (Soddy and Berry, 1910; Saltsburg et al., 1967; Thomas, 1980). A useful parameter is the energy accommodation coefficient, which is a measure of the fraction of the kinetic energy lost by an incident molecule before it is reemitted. The laboratory experiments have shown that molecules striking clean surfaces have low energy accommodation coefficients, and are typically reflected with a quasi-specular angular distribution (Thomas ,1980; Moe et al., 1998). In contrast, molecules striking contaminated surfaces have high accommodation coefficients and are reemitted with a diffuse angular distribution. Laboratory experiments also have shown that accommodation coefficients of many gases on contaminated metal surfaces are independent of the metal used (Stickney and Hurlbut, 1963; Kostoff et al., 1967).

Early calculations of satellite drag coefficients based on laboratory measurements were made by Izakov (1965) and Cook (1965, 1966). Their papers led to the widespread use of a fixed drag coefficient, $C_d = 2.2$, for satellites of compact shapes. This had the advantage of simplifying orbital calculations. In spite of the ingenuity of these early workers, their results were limited by dependence on data coming from laboratory experiments on clean surfaces. In particular, Goodman's formula (Goodman, 1964, 1967) for the accommodation coefficient (quoted by Cook, 1965, 1966) does not apply to the conditions on satellite surfaces in orbit. At first, drag coefficients for the accelerometer-carrying CHAMP satellite were calculated using the early work of Cook and the assumption of hyperthermal free-molecular flow (Bruinsma et al., 2004). This produced drag coefficients that were too low (Marcos, 2005; Bowman et al, 2007; Sutton, 2009). In contrast, Sentman's (1961a, 1961b) analysis of forces on a satellite surface is appropriate to the reality that the surfaces of orbiting satellites are contaminated. Sentman-based calculations produce drag coefficients between 3 and 4 for long attitude-controlled satellites such as CHAMP (Sentman, 1961b; Bowman et al., 2007).

For half a century, satellite experimenters have been investigating the drag interaction with satellite surfaces (Moe, 1966; Karr, 1969; Reiter and Moe, 1969; Beletsky, 1970; Imbro et al., 1975; Ching et al., 1977; Gregory and Peters, 1987; Bowman and Moe, 2005; Pardini et al., 2010; Koppenwallner, 2011; Pilinski, et al., 2011a). Satellite measurements by pressure (density) gauges and mass spectrometers have shown that the surfaces of satellites become partly covered by adsorbed atomic oxygen and its reaction products (Moe and Moe, 1969; Hedin et al., 1973; Moe et al., 1998). This partial coverage varies continuously as the satellite moves around its orbit, causing gradual variation

of the drag coefficient. The surface coverage varies much more slowly than the ambient molecular density and composition, so the drag coefficient of a particular satellite varies only slowly during the orbit (Moe et al., 1995, 1998). Whenever we measure a drag coefficient using the orbital decay of satellites in orbits of low eccentricity, we are actually measuring an average around many orbits.

Figure 1 shows the drag coefficients of satellites of four compact shapes in low-Earth orbits, calculated by introducing the energy accommodation coefficients measured in orbit into Sentman's (1961a) analysis. This figure applies to times of low solar activity in the 1960s and 1970s (Moe and Moe, 2005). Studies reported below in Section 3 suggest that the density of atomic oxygen at a specific altitude in the thermosphere has been decreasing secularly because of increasing atmospheric concentrations of carbon dioxide. If the concentration of atomic oxygen at a specific altitude in the thermosphere at sunspot minimum were 20% lower in the current epoch than it was in the 1960s, when the paddlewheel satellites measured accommodation coefficients at sunspot minimum (Moe, et al., 1995), then the accommodation coefficient at 300 km might now be several percent lower. In such a case, the drag coefficient of a sphere could be a few percent higher than it was at the sunspot minimum in the 1960s.

The issue of a long-term secular change in drag coefficients could be settled by a new research program in which attitude-controlled, spinning paddlewheel satellites would be flown in eccentric orbits (Pilinski et al., 2011b). Such satellites, combining both spin and orbital decay measurements, could simultaneously measure both air density and drag coefficient. Thus, paddlewheel satellites can measure absolute air densities.

Notice that, in Figure 1, except below 240 km for spherical satellites, and below 200 km for a flat plate, the drag coefficients are above 2.2. In fact, for long attitude controlled satellites, the drag coefficient will attain values above 3.0 (Sentman, 1961b; Bowman, et al., 2007), and will show a much stronger dependency on temperature and molecular mass of the atmospheric particles (Doornbos, et al., 2010). Looking ahead, the constellation of three SWARM satellites, which resemble CHAMP, will soon be flown. A way of avoiding drag coefficient problems (as well as difficulties in determining stormtime winds) is to fly several small satellites carrying density gauges and paddlewheels near the SWARM constellation. At geomagnetically quiet times, these small accompanying satellites would inexpensively measure absolute densities in the regions through which the larger satellites fly. By combining the data from the density gauges with the data from the SWARM accelerometers, the in-track wind can be inferred. This would help to resolve the long-standing problem of measuring accurate densities during geomagnetic storms (Moe and Moe, 1992).

3. Density Trends

After comparing the orbital decay of many satellites over many decades, several analysts have reported a long-term decrease in the thermospheric density (Keating et al., 2000; Marcos et al., 2005; Lean et al., 2006; Qian et al., 2006; Emmert et al., 2008). This decrease in density has been attributed to a cooling and shrinking of the mesosphere and thermosphere (Dickinson, 1984). This effect, which is observed in the thermosphere, has a counterpart in the descent of the F-region ionosphere (Laštovička, et al., 2006).

A likely physical mechanism is infra-red radiative cooling by the increasing densities of carbon dioxide and methane. A much smaller density decrease has been reported at sunspot maxima than at sunspot minima (Marcos et al., 2005). Emmert et al. (2008) have also reported that the density decrease is smallest in January, and largest, at about 4% per decade, in November.

A much greater density decrease has been reported at the 2008 solar minimum. Thermospheric models have been unable to predict the magnitude of this decrease, even when carbon dioxide was factored in (Emmert et al., 2010; Solomon et al., 2010). Solomon et al. (2010) believe that most of the density decrease can be attributed to reduced solar ultraviolet emissions, while Moe and Moe (2011) think that the difficulty is more fundamental, involving how energy sources and sinks are built into the semi-empirical, operational density models: The UV contribution is overestimated by the neglect of eddy diffusion which carries energy from the thermosphere down into the mesosphere, while the corpuscular energy source in the ever-present solar wind is not well represented by A_p or K_p. Qian, et al. (2009) are applying the three-dimensional physics of a general circulation model to drag and TIMED/GUVI data to learn how turbulent mixing from below contributes to the seasonal variation in the thermosphere. Budzien, et al. (2010) are using the RAIDS instrumentation on the Space Station to measure the composition and temperature in the lowest thermosphere. These fundamental investigations should soon make it possible to improve the operational density models.

The density trend calculations cited above assumed that satellite drag coefficients are independent of satellite shape, altitude, time in the sunspot cycle, and concentration of atomic oxygen in the thermosphere. All of these assumptions may be seriously flawed, as the references in Section 2 indicate. Quantitative calculations of the changes in density should include the use of realistic drag coefficients and their variations (Moe and Moe, 2011). If new paddlewheel satellites are flown (Pilinski, et al., 2011b), it will be possible to measure how much drag coefficients and thermospheric densities have actually changed since the 1960s.

4. Calibration of Mass Spectrometers and Pressure (Density) Gauges

Early in the Space Age, mass spectrometers and pressure (density) gauges were calibrated in the laboratory by introducing measured amounts of non-reactive gases into the instruments and then measuring the resulting output currents. The densities measured in orbit by these instruments were roughly half of the densities measured by orbital decay (Hedin and Nier, 1966; Mauersberger, et al., 1967; Newton, 1969; Nier, 1972).

In those days, the differential equations describing the processes in gauges and mass spectrometers did not include adsorption or desorption, so the instruments were carried on spinning spacecraft to separate "outgassing" (desorption of gases present at launch) from the atmospheric signal (Harris and Spencer, 1965; Spencer, et al., 1966; Nier, 1967). The addition of adsorption and desorption to the differential equations reduced the discrepancy between these instrumental measurements and drag-based measurements (Moe and Moe, 1969; Hedin, et al., 1973). Laboratory experiments showed that atomic oxygen adsorbs onto the surfaces of many materials (Riley and Giese, 1970; Wood, 1971). Additional evidence came from the rocket flights of a cryogenically-cooled mass spectrometer and an uncooled instrument of the same design, confirming that density and composition measurements of uncooled instruments can be improved by including adsorption and surface chemical reactions in the processes considered (Offermann and Grossmann, 1972). After space experiments had demonstrated the reality that adsorption and surface reactions do occur in space, the satellite experimenters performed laboratory experiments confirming these same processes (Lake and Nier, 1973; Lake and Mauersberger, 1974).

By comparing OGO-6 mass spectrometric data with adsorption theory, Hedin et al. (1973) showed that nearly all of the carbon contaminants had been burned out of the mass spectrometer after two weeks in orbit. After that time, the measured molecular oxygen could be attributed to atomic oxygen in the ambient atmosphere. This simplified the problem of deducing ambient species from measurements by uncooled mass spectrometers. With this understanding, experimenters compared the density and composition measurements from four satellites on occasions when any pair of satellites

passed near each other (Trinks, et al., 1977). The mean differences among the instruments for molecular nitrogen, atomic oxygen, and helium ranged up to 24 %, 18 %, and 75 %, respectively. A more detailed comparison among the closed-source (NACE) and open-source (OSS) mass spectrometers and the Bell-MESA accelerometer on the Atmosphere Explorer C satellite by Killeen, et al. (1989) showed that the total mass density ratio OSS/MESA ranged from about 0.1 to 2, with a mean that varied with altitude and an rms value of about 0.3; and the ratio NACE/MESA was 1.07 ± 0.12.

5. Calibration of Accelerometers

Micro-g accelerometers can be calibrated on the ground, but the side forces in a one-g environment, among other factors, introduce uncertainties. Therefore, the first accelerometer flown, a Bell MESA, was also calibrated in orbit by using the principle of the centrifuge, by placing the accelerometer on a rotating table on the LOGACS satellite (Pearson, 1973). Stanford University's more advanced accelerometer, DISCOS (Disturbance Compensation System), consisted of a proof mass and a surrounding shell containing capacitive sensors. The Triad satellite containing DISCOS was then kept in a drag-free orbit using gas jets. Ground calibrations were performed with a caging rod and with precision shims. In-orbit calibrations were performed by comparing the signals produced when the proof mass was released in orbit with the results of the ground calibrations. The several ground-based and space-based methods of calibration used on DISCOS are described in detail in Moe, et al. (1976), and in the references of that paper.

Accelerometers flown more recently, such as STAR flown on CHAMP and SuperSTAR flown on GRACE, consist of a proof mass surrounded by an instrumented cage. As with DISCOS, the ground calibration was considered inaccurate. However, the CHAMP and GRACE satellites are equipped with highly accurate satellite-tracking instrumentation, using the Global Positioning System (GPS) and the Satellite Laser Ranging (SLR) network. This tracking data can be used to calibrate the accelerations from the STAR and SuperSTAR instruments to a relatively high accuracy, even detecting drifts and jumps over time. Bruinsma, et al. (2004) concluded that their STAR calibration error was only 2%, but that the error in their drag coefficient was 5 to 10 %. Therefore, for these missions, the influence of the accelerometer calibration on the density error is well below that of the drag coefficient uncertainty.

6. Spacecraft Geometry

Unfortunately, the publicly reported dimensions of satellites can contain large errors, which will hinder the computation of accurate physical drag coefficients and densities. Uncertainties in the area can be especially large when the experimenters have added antennas, sensors, booms and baffles to the spacecraft exterior, such as on CHAMP. The use of a panellized model of this satellite (Lühr, et al., 2002) will result in a frontal area that is 37% smaller than that specified by the satellite manufacturer, in which all instruments and other appendages are present. Bruinsma and Biancale (2003) have created and applied a modified simplified panel model, in which the discrepancy was reduced to 14%. Recently, as part of an ESA study (Doornbos, et al., 2009), a new detailed 3D model of CHAMP was built in the ANGARA analysis software (Fritsche and Klinkrad, 2004), based on detailed drawings from the manufacturer. The maximum frontal area discrepancy when compared with the drawings from the manufacturer was still 7%. Even for GRACE, which has a simpler geometry than CHAMP, discrepancies between specified frontal areas were up to 7%, depending on the viewing geometry.

Moe and Bowman (2005) reported similar uncertainties for spherical satellites containing solar cells or reflectors. Surface composition and surface roughness have only a one to three percent effect

on drag coefficients near 300 km, but solar cells and objects attached to the surfaces of spherical satellites appear to increase C_d by 3 to 10 %, while the deep indentations in the spherical surface of the laser retroreflector satellite GFZ-1 seemed to increase its C_d by as much as 30 % (Moe and Bowman, 2005; Pardini, personal communication, 2008).

These uncertainties increase the potential errors in calculating densities, accommodation coefficients, and drag coefficients from satellite drag data. Pilinski et al. (2011a) used Monte Carlo calculations to investigate the effect of surface modifications on the drag coefficients of spheres**.** They did not observe large effects of the solar cells attached to satellite surfaces. They did find that the Starshine Satellites retained their attachment rings in orbit, so that Moe and Bowman (2005) underestimated their areas and overestimated their drag coefficients. Guidamean (personal communication, 2009) revealed that the canister from which the Optical Calibration Sphere (OCS) emerged had remained attached to the sphere, so OCS had a larger area than had originally been assumed by Pardini, et al. (2010). They therefore decided to remove that satellite from their final calculations. These recent results show that modified spheres often have a different drag because of a simple change in area, not because of some special effect of flat solar cells attached to a spherical surface.

7. Solar Radiation Pressure Effect on Satellite Drag Measurements

When deriving densities from satellite drag observations, it is important to take accelerations due to radiation pressure into account. Above about 400 km at solar minimum, and about 600 km at solar maximum, the density will have decreased sufficiently for the magnitude of the drag acceleration to drop below that due to radiation pressure. The two kinds of forces can point in different directions, and are complicated by shadowing and the reflective properties of the spacecraft.

The modeling of the effects of radiation pressure accelerations is a complex topic. Nevertheless, many skilled analysts and experimenters have studied this problem from the earliest days of space flight. Fifteen papers published before 1962 were cited in a section on solar radiation pressure in the Flight Performance Handbook for Orbital Operations, edited by R. W. Wolverton, and published by Wiley in 1963. Spacecraft eclipses were analyzed in the subsequent section of that handbook. Originally, most attention was devoted to astronomical perturbation theory. Over the decades, more and more sophisticated analyses have been published, but they often deal with GPS orbits or geosynchronous orbits, where radiation pressure is of overriding importance. A fine example is Ziebart (2004). An effort to "tune" a radiation pressure model at 600 km is described in Rim, et al. (2007). Two examples of using radiation pressure models in the evaluation of Iridium orbits near 700 km are provided by Puderbaugh, et al. (2002) and Gottlieb, et al. (2001). Doornbos, et al. (2002) made an analysis for the precise orbit determination of ERS-2 and Envisat satellites at about 800 km altitude. Similar models are in use for the density determination from CHAMP and GRACE accelerometer observations as well.

A fraction of the sunlight impinging on the spacecraft surfaces can be absorbed; other fractions can be reflected diffusely and specularly. The absorptive and reflective properties of the satellite rarely are measured or reported by the manufacturer (Ziebart, 2004). Even if they were reported, they would change in orbit, as we learned from the flight of the Long Duration Exposure Facility (LDEF) (Murr and Kinnard, 1993; Levine, 1991). Radiation pressure causes particular difficulties for deriving densities from orbit observations of spacecraft debris (Picone, et al., 2005).

Sunlight strikes the satellite only when it is outside the Earth's shadow, so solar radiation pressure effects partly cancel on opposite sides of the orbit if the orbit stays in the sunlight. However, radiation pressure can also have large secular effects on the orbit, which can exceed that of drag, especially

when the orbit is eccentric and passes through eclipses (see for example, Kozai, 1961; Milani, et al., 1987).

When processing accelerometer measurements made during eclipse transitions, subtle phenomena such as the atmospheric absorption and refraction of sunlight (Vokrouhlický, et al., 1994), and the impact of the oblateness of the Earth (Vokrouhlický, et al., 1996, Adhya, et al., 2004) become important to consider.

Sunlight reflected from the Earth (albedo) and infrared radiation emitted by the Earth are large secondary sources of radiation pressure that bring their own modeling difficulties. Both effects are of similar magnitude, at about 20-30% of the solar radiation pressure in the altitude range that is of interest for drag observations (Milani, et al., 1987). However, the local amount of reflection and emission is determined by variable properties such as the depth and character of cloud cover and the extent of snow and sea ice cover. These effects are difficult to calculate or predict accurately. The average albedo is about 30 %, but the local albedo can vary from 92 % over large and thick cumulonimbus clouds to 7 % over a cloudless ocean (Conover, 1965).

Earth albedo and infrared radiation primarily cause accelerations in the radial direction, instead of the along-track direction that is most important for drag. Therefore, they are of minor concern when deriving density data from accelerometer measurements.

Pardini, et al. (2010) used the computer program, SATRAP, to evaluate the effect of radiation pressure on deduced drag coefficients near 500 and 600 km at sunspot maximum. The radiation pressure was varied to estimate the effect of differing albedo and infrared emission. Uncertainty in these effects had a negligible effect on the drag coefficients deduced from the satellites studied.

The absorption of sunlight by the spacecraft will cause it to heat up. Eventually, this heat will be reemitted into space in the form of infrared radiation. This will generally happen in an anisotropic fashion, causing an additional acceleration. This anisotropic thermal re-radiation acceleration is even more difficult to model than the other effects discussed above, because it depends on the emissivity and thermal control properties of the spacecraft. Its magnitude is estimated to be at a level of about 5-10% of the solar radiation pressure for most thermally controlled satellites (Ziebart, et al., 2005).

8. Calibration of Ultraviolet Spectrometers

The ultraviolet spectrometric sensors, SSUSI and SSULI, will be used on the DMSP satellites to monitor the density by adding the measured constituents. Ultraviolet spectrometers have many sources of error: Uncertainties in the solar UV spectrum, photoabsorption cross sections of atmospheric gases, photoelectron flux models, radiation transfer models, lifetimes of excited states, calibration, and decay of the calibration with time. If there are forbidden transitions within the spectral region of interest or at shorter wavelengths, then collisional deactivation will exacerbate the problem of calculating the spectrum for comparison with the observational data. Many of these problems have been discussed and evaluated by Budzien et al. (1994), Torr et al. (1993), Huffman (1992), and Rees (1990). In some of the wavelengths chosen for comparison in these papers, the disagreements between theory and experiment ranged from approximately 20 % to 100 %.

A particularly informative comparison of theoretical and experimental spectra was provided by the Atlas-1 experiment, which was discussed in a collection of papers in the Geophysical Research Letters, Vol. 20, no. 6, March 19, 1993, pp. 487-534. In the ATLAS-1 experiment, the theoretical spectrum was **not** adjusted ("tuned") to fit the experimental data. At most wavelengths, the theoretical and measured spectra agreed within a factor of two.

Marcos (2005) has used STAR accelerometer measurements from the CHAMP and GRACE satellites to evaluate the UV spectrometric measurements of the GUVI instrument on the TIMED satellite. First, he corrected the CHAMP and GRACE drag coefficients. He then calculated ratios of densities derived from the GUVI spectrometers and the STAR accelerometers. Marcos found that the ratios ranged from 0.6 to 1.6. This range is well within the range of far UV emission accuracies of 20 to 100 % in Table 1.

A general circulation model has been introduced into the effort to validate UV spectrometric measurements (Meier, et al., 2005). General circulation models have had great success in explaining the response of the thermosphere to geomagnetic storms (Fuller-Rowell, et al., 1990, 1994). Yet these models do not, as yet, represent well the energy and momentum sources provided by coupling with the mesosphere, and by coupling with the magnetosphere at geomagnetically quiet times. The general features of the UV data are well represented by the general circulation model, but the model and the UV data lack the precision of orbital drag data: Compare the error estimates in Table 1 with discrepancies illustrated in the papers by Marcos (2005), and Meier, et al., (2005).

9. Density Models

Previous versions of CIRA have described the physical concepts and the differential equations from which the semi-empirical thermospheric models have been developed. Pardini et al. (2011) have briefly discussed the physical ideas and data sets that were used in constructing and improving the various fast-running, semi-empirical models that are in wide operational use. The Jacchia (1970) model is an example of such a semi-empirical model. The constants in these models often have been derived from satellite drag measurements in which the drag coefficient has been assumed to be independent of altitude and time in the sunspot cycle. This assumption leads to altitude-dependent biases in both the density measurements and models. The instrumental measurements used in constructing the MSIS models can also introduce biases.

Absolute densities are rarely needed when using operational models for orbit fitting, because the drag coefficient is simply adjusted to force the model to fit the tracking data. However, when comparing drag-based models with measurements by other kinds of instruments, it is necessary to calculate absolute densities from the model. An evaluation of the biases in the Jacchia 71 and MSIS 90 thermospheric models was carried out by Chao et al. (1997). As examples of the kinds of biases that exist in some operational density models, we show the results of two later studies: Table 2 gives the conclusions of a detailed analysis of the bias in the J70MOD (a modification of the Jacchia 70 Model by Bowman) for sunspot minimum and maximum conditions (Bowman and Moe, 2005); Table 3 compares the biases in two different modifications of the Jacchia model (J70MOD and JB2006) for sunspot maximum conditions (Pardini et al, 2010). In his new JB2008 density model, Bowman has considerably reduced the bias at 400 km altitude (Bowman et al. 2008b).

Absolute densities at sunspot maximum and minimum can be calculated from the J70MOD by reducing the model density at low and middle latitudes by the percentages in Table 2. The long-term density trends discussed in Section 3 suggest that model densities might now be reduced even more at sunspot minimum. This uncertainty could be resolved by flying paddlewheel satellites, which are capable of measuring absolute densities.

At high geomagnetic latitudes on the dayside, energy enters the thermosphere continuously through the dayside cusps of the magnetosphere (Heikkila and Winningham 1971; Olson 1972, Shepherd and Thirkettle 1973; Olson and Moe 1974; Moe and Moe 2008). At certain places and times this energy source can cause the air density to exceed the Jacchia model density, since the Jacchia model had only an ultraviolet energy source at geomagnetically quiet times (See Figure 3 of Moe and

Moe (2008)). This density bulge was first identified by Jacobs (1967). When the correct drag coefficients have been established for CHAMP and GRACE, data from these satellites and modelling of the high latitude energy sources can be used to correct thermospheric models at quiet times.

Several investigators have performed studies that can improve thermospheric models:

Faivre, et al. (2006) have studied the midnight temperature maximum phenomenon at Arequipa; Liu et al. (2005) have evaluated the equatorial thermospheric mass-density anomaly; Forbes, et al., 2008 identified solar terminator waves in the CHAMP data; while Newell and Meng (1988) and Liou et al. (1999) have documented the contributions of the plasmasphere and magnetospheric tail to the dayside auroral heating at quiet times.

Since very early in thermospheric modeling, the geomagnetic planetary amplitude, a_p , has been used to represent the magnetospheric energy source, and the solar radio noise at 10.7 cm (F10.7) has been used to represent the UV source. Tobiska (2001) and Tobiska et al. (2008) have proposed replacing the F10.7 cm radio noise index with indices based on direct space-based measurements of the solar UV radiance in spectral regions that energize directly the key regions and processes in the upper mesosphere and thermosphere. These new indices have been shown (Bowman et al., 2008a) to provide a better representation of the solar ultraviolet energy source. Bowman et al. (2008b) have now begun to use the ring current index Dst in addition to a_p to represent the effect of geomagnetic energy on the thermosphere.

Static diffusion models and other fast-running operational models take no account of the combined effect of large-scale horizontal and vertical winds (advection and convection), which can redistribute the constituents on constant pressure levels. This simplification introduces a bias into operational models. May (1973) demonstrated that static diffusion models do not represent correctly the dawn/dusk ratio of molecular oxygen. Modali et al. (1976) showed that the values of atomic oxygen and molecular nitrogen near 400 km are consistent with a Jacchia model at sunset, but vary erratically about the Jacchia model at sunrise. Recent measurements near 100 km are incompatible with static diffusion models (Broadfoot and Gardner, 2001; Culot, 2004). During geomagnetic storms, the combination of strong horizontal and vertical thermospheric winds increases modeling difficulties by changing the composition quite dramatically (Obayashi and Matuura, 1971; Hecht et al., 1989; Richards, 2002). The winds which cause compositional changes during storms can interfere with the analysis of measurements (Moe and Moe, 1992; Moe et al., 2004).

General circulation models (which run more slowly than the operational models described above) include three-dimensional motions, so they have had great success in representing the wind systems that redistribute atmospheric species both during geomagnetic storms, and at quiet times (Fuller-Rowell et al., 1990, 1994). Being based on fundamental physics, these models require input of all the sources and sinks of energy. Since some of these sources and sinks are poorly known, the models themselves are presently limited in their accuracy.

Renewed efforts to compare measurements near the interface of the mesosphere and thermosphere with theory (Qian, et al., 2009; Budzien, et al., 2010; Moe and Moe, 2011) can improve the modeling of that important region. Continuation of the efforts to intercompare simultaneous measurements throughout the thermosphere by different instruments (Trinks, et al., 1977; Marcos, et al., 1977; Killeen, et al., 1989; Richards, 2002; Moe, et al., 2004; Marcos, 2005) can improve our understanding of the entire thermosphere.

10. Summary

Outstanding issues affecting thermospheric measurements and models are reviewed with reference to their historical development and the present state of knowledge. Efforts to advance our understanding of the roles of drag coefficients, density trends, radiation pressure, instrument calibrations, and high-latitude energy sources are described**.** Possible causes for the unexpectedly large density decrease at the 2008 solar minimum are discussed. Many new and improved methods of thermospheric measurement are presented. They will provide a data base that will support the development of improved density models.

References

Adhya, S., Sibthorpe, A., Ziebart, M., Cross, P. Oblate earth eclipse state algorithm for low-earth orbiting satellites. Journal of Spacecraft and Rockets, 41(1):157–159, 2004.

Beletsky, V. V. An estimate of the character of the interaction between the airstream and a satellite. Kosmicheskie issledovaniya 8, 206-217, 1970. (In Russian).

Bowman, B. R., Moe, K. Drag coefficient variability at 175-500 km from the orbit decay analysis of spheres. Paper AAS 2005-257, American Astronautical Society Publications Office, San Diego, CA, 2005.

Bowman, B. R., Marcos, F. A., Moe, K., Moe, M. M. Determination of drag coefficient values for CHAMP and GRACE satellites using orbit drag analysis. Paper AAS 2007-259, American Astronautical Society Publications Office, San Diego, CA, 2007.

Bowman, B. R., Tobiska, W. K., Kendra, M. J. The thermosphere semiannual density response to solar EUV heating. J. Atm. Solar-Terr. Phys., 2008a, doi:10.1016/j.jastp. 2008.04020.

Bowman, B. R., Tobiska, W. K., Marcos, F. A., Huang, C. Y., Lin, C. S., Burke, W. J. A new empirical thermospheric density model JB2008 using new solar and geomagnetic indices. Paper AIAA 2008b-6438, American Inst. of Aero. and Astro, Reston, Va.

Broadfoot , A. L., Gardner, J. A. Hyperspectral imaging of the night airglow layer from the Shuttle: A study of temporal variability. J. Geophys. Res. 106, 24,795-24,811, 2001.

Bruinsma, S. L., Biancale, R. Total densities derived from accelerometer data. J. Spacecraft and Rockets 40, 230-236, 2003.

Bruinsma, S., Tamagnan, D., Biancale, R. Atmospheric densities derived from CHAMP / STAR accelerometer observations. Plan.and Space Sci. 52, 297-312, 2004.

Budzien, S. A., Feldman, P. D., Conway, R. R. Observations of the far UV airglow by the UV Limb Imaging Experiment on STS 39. J. Geophys. Res. 99, 23,275-23,287, 1994.

Budzien, S. A., Bishop, R. L., Stephan, A. W., Christensen, A. B., McMullin, D. R. Atmospheric remote sensing on the International Space Station. EOS, Trans. Am. Geophys. U. 91 (No. 42) 19 Oct. 2010.

Chao, C. C., Gunning, G. R., Moe, K, Chastain, S. H., Settecerri, T. J. An evaluation of Jacchia 71 and MSIS 90 atmosphere models with NASA ODERACS decay data. J. Astronaut. Sci 45, 131-141, 1997.

Ching, B. K., Hickman, D. R., Straus, J M. Effects of atmospheric winds and aerodynamic lift on the inclination of the orbit of the S3-1 satellite. J. Geophys. Res. 82, 1474-1480, 1977.

Conover, J. H., Cloud and terrestrial albedo determinations from TIROS satellite pictures. J. Appl. Meteor., 4, 378-386., 1965.

Cook, G. E. Satellite drag coefficients. Plan. Space Sci. 13 , 929-946, 1965.

Cook, G. E. Drag coefficients of spherical satellites. Ann. de Geophys. 22, 53-64, 1966.

Culot, F. Thesis, Study of Radiation at 557.7 and 630.0 Nanometers, University of Grenoble. http://culot.org/public/Manuscrit/node5.html. 2004 (in French).

Dickinson, R. E. Infrared radiative cooling in the mesosphere and lower thermosphere. J. Atmos. Terr. Phys., 46, 995-1008, 1984.

Doornbos, E., Scharroo, R., Klinkrad, H., Zandbergen, R., Fritsche, B., Improved modelling of surface forces in the orbit determination of ERS and Envisat. Canadian Journal of Remote Sensing, 28(4), 535–543, 2002.

Doornbos, E., Förster, M.., Fritsche, B., van Helleputte, T., van den IJssel, J., Koppenwallner, G., Lühr, H., Rees, D., Visser, P., Kern, M.. Air density models derived from multi-satelllite drag observations, Technical report DEOS/TU Delft, Delft, The Netherlands, 2009.

Doornbos, E., van den IJssel, J., Lühr, H., Förster, M. and Koppenwallner, G., Neutral density and crosswind determination from arbitrarily oriented multiaxis accelerometers on satellites. Journal of Spacecraft and Rockets 47, 580-589, 2010

Emmert, J. T., Picone, J. M., Meier, R. R. Thermospheric global average density trends, 1967-2007, derived from orbits of 5000 near-Earth objects. Geophys. Res. Let. 35, L05101, doi:10.1029/2007GL032809, 2008.

Emmert, J. T., Lean, J. L., Picone, J. M. Record-low thermospheric density during the 2008 solar minimum, Geophys. Res. Lett. 37, L12102, doi:10.1029/2010GL043671, 2010.

Faivre, M., Meriwether, J. W., Fesen, C. G., Biondi, M. A. Climatology of the midnight temperature maximum phenomenon at Arequipa, Peru. J. Geophys, Res., 111, A06302, 2006.

Forbes, J., Bruinsma, S., Miyoshi, Y., Fujiwara, H., A solar terminator wave in thermosphere neutral densities measured by the CHAMP satellite. Geophysical Research Letters 35, L14802, doi:10.1029/2008GL034075, 2008

Fritsche, B., Klinkrad, H., Accurate prediction of non-gravitational forces for precise orbit determination, part II: Determination of perturbing forces and torques in an orbital environment. AIAA/AAS Astrodynamics Specialist Conference and Exhibit, 16–19 August 2004, Providence, Rhode Island, AIAA 2004-5462, 2004.

Fuller-Rowell, T. J., Rees, D., Tinsley, B. A., Rishbeth, H., Rodger, A. S., Quegan, S., Modelling the response of the thermosphere and ionosphere to geomagnetic storms: Effects of a mid-latitude heat source. Adv. Space Res. 10, 215-224, 1990.

Fuller-Rowell, T. J., Codrescu, M. V., Moffett, R. J., Quegan, S. Response of the thermosphere and ionosphere to geomagnetic storms. J. Geophys. Res. 99, 3893-3914, 1994.

Goodman, F. O., Fourth Intl. Symposium on Rarefied Gas Dynamics, Academic, New York, 1964.

Goodman, F. O. Preliminary results of three-dimensional hard-sphere theory of scattering of gas atoms from a solid surface, in Proceedings of the 5th Intl. Symposium on Rarefied Gas Dynamics, Academic, New York, 1967, pp. 35-48.

Gottlieb, R. G., Sponagle, S. J., Gaylor, D. E., Orbit determination accuracy requirements for collision avoidance, AAS 01 181, American Astronautical Society Publications Office, San Diego, CA , 2001.

Gregory, J. C., Peters, P. N. A measurement of the angular distribution of 5 eV atomic oxygen scattered off a solid surface in Earth orbit, in: Proceedings of the 15th Intl. Symposium on Rarefied Gas Dynamics, Ed. by V. Boffi and C. Cercignani, Vol. 2, B. G. Teubner, Stuttgart, Germany, pp. 644-654, 1987.

Guidamean, K. Personal communication, 2009.

Harris, I., Spencer, N. W. in W. N. Hess (Ed.), Introduction to Space Science, Gordon and Breach, N. Y., 1965, p. 112.

Hecht, et al. Deducing composition and incident electron spectra from ground-based auroral optical measurements: variations in oxygen density. J. Geophys. Res. 94, 13,553, 1989.

Hedin, A. E., Hinton, B. B., Schmitt, G. A. Role of gas-surface interactions in the reduction of Ogo 6 neutral particle mass spectrometer data. Geophys. Res. 78, 4651-4668, 1973.

Hedin, A. E., Nier, A. O., A determination of the neutral composition, J. Geophys. Res. 71, 4121-4131, 1966.

Heikkila, W. J., Winningham, J. D. Penetration of magnetosheath plasma to low altitudes through the dayside magnetospheric cusps. J. Geophys. Res. 76, 883-891, 1971.

Hinteregger, H. E., Hall, L. A. Thermospheric densities and temperatures. Space Res. IX, North Holland, Amsterdam, 1969.

Huffman, R. E. Atmospheric Ultraviolet Remote Sensing, Academic Press, Boston. 1992.

Imbro, D. R., Moe, M. M., Moe, K. On fundamental problems in the deduction of atmospheric densities from satellite drag. J. Geophys. Res. 80, 3077-3086, 1975.

Izakov, M. N. Some problems of investigating the structure of the upper atmosphere and constructing its model. Space Res. 5, 1191- 1213, 1965.

Jacchia., L. G. New static models of the thermosphere. Smithsonian Astrophys. Obs., Special Rep. 313, Cambridge, MA, 1970.

Jacobs, R, L. Atmospheric density derived from the drag of eleven low altitude satellites. J. Geophys. Res. 72, 1571-1581, 1967.

Karr, G. R. A study of effects of the gas-surface interaction on spinning convex bodies with application to satellite experiments, Rep. R-435, Coord. Sci. Lab., Univ. of Ill., Urbana, 1969.

Keating, G. M.., Tolson, R. H., Bradford, M. S. Evidence of long-term global decline in the Earth's thermospheric densities apparently related to anthropogenic effects. Geophys. Res. Let.27, 1523-1526, 2000.

Killeen, T. L., Burns, A. G., Kennedy, B. C., Roble, R. G., Marcos, F. A. Feasibility Study for an Atmospheric Density Specification Satellite. GL-TR-890081, Geophysics Laboratory, Hanscom AFB Massachusetts, 1989, p. 42.

Koppenwallner, G. Satellite aerodynamics and determination of thermospheric density and wind. 27th Intl. Symp. Rarefied Gas Dynamics, 2010, AIP. Conf. Proc. 1333, 1307-1312 (2011); doi:10.1063/1.3562824.

Kostoff, R.N. Anderson, J.B., Fenn, J.B. Measurements of momentum accommodation of gas molecules at surfaces. In H. Saltsburg, J. N. Smith, and M. Rogers, editors, Fundamentals of Gas-Surface Interactions, Symposium, San Diego, Dec. 1966, pages 512–521. Academic Press, New York., 1967.

Kozai, Y., Effects of Solar Radiation Pressure…Smithsonian Astrophysical Observatory, Cambridge, MA, Sp. Rep. 56, 1961, pp. 25-33.

Lake, L. R., Mauersberger, K. Investigation of atomic oxygen in mass spectrometer ion sources. Intl. J. Mass Spectrom. and Ion Phys. 13, 425-436, 1974.

Lake, L. R., Nier, A. O. Loss of atomic oxygen in mass spectrometer ion sources. J. Geophys. Res. 78, 1645-1653, 1973.

Laštovička, J., Akmaev, R., Beig, G., Bremer, J., Emmert, J. Global change in the upper atmosphere. Science, 314(5803):1253–1254, 2006.

Lean, J. L., Picone, J. M., Emmert, J. T., Moore, G. Thermospheric densities derived from spacecraft orbits: Application to the Starshine satellites. J. Geophys. Res. 111, A04301, doi:10.1029/2005JA011399, 2006.

Levine, A. S. (Editor), LDEF – 69 Months in Space. First post-retrieval symposium. NASA, Washington, D. C., 1991.

Liou, K., Newell, P. T., Meng, C.-I., Sotirelis, T., Brittnacher, M., Parks, G., Source region of 1599 MLT auroral bright spots…J. Geophys. Res. 104, A900290, 1999.

Liu, H., Luehr, H., Henize, V., Koehler, W. Global distribution of the thermospheric total mass density derived from CHAMP. J. Geophys. Res. 110, A04301, 2005.

Lühr, H., Grunwaldt, L., Förste, Ch., CHAMP reference systems, transformations and standards, GFZ-Potsdam, CH-GFZ-RS-002, 2002.

Majeed, T., Strickland, D. J., Link, R. Analysis of AIS dayglow and nightglow limb radiances, Tech. Rep. on Contract no. F19628-92-C-0016, Computational Physics Inc., Fairfax, Virginia, 1993.

Marcos, F. A., Philbrick, C. R., Rice, C. J. Correlative satellite measurements of atmospheric mass density by accelerometers, mass spectrometers, and ionization gauges, in Space Research XVII, Pergamon, Oxford 1977, pp. 329-333.

Marcos, F. A. New measurements of thermospheric neutral density: A review, Paper AAS 05-251. American Astronautical Society Publications Office, San Diego, CA, 2005.

Marcos, F. A., Wise, J. O., Kendra, M. J., Grossbard, N. J., Bowman, B. A. Detection of a long-term decrease in thermospheric neutral density. Geophys. Res. Let. 32, L04103, doi:10.1029/2004GL021269, 2005.

Mauersberger, K., Muller, D., Offermann, D., von Zahn, U., in R. L. Smith-Rose, (Ed.), in Space Research VII, North-Holland Publ. Co., Amsterdam, 1150-1158. 1967.

May, B. Molecular oxygen density in the lower thermosphere. Space Research XIII, 243, 1973.

Meier, R. R., et al. First look at the 20 November 2003 superstorm with TIMED/GUVI: Comparisons with a thermospheric global circulation model. J. Geophys. Res. 110, A09S41, doi:19.1029/2004JA010990, 2005.

Milani, A., Nobili, A.M., Farinella, P., Non-gravitational perturbations and space geodesy, Adam Hilger, Bristol, 1987.

Modali, S.B., Thomas, R. W. L., Chapman, R. D., Thomas, R. J. OSO-7 measurements of atomic oxygen and molecular nitrogen densities … J. Geophys. Res. 81, 6203-6206, 1976.

Moe, K. Absolute atmospheric densities determined from the spin and orbital decays of Explorer VI. Planet. Sci. Planet. Sci, 14, 1065-1075, 1966.

Moe, K. The mean molecular mass. Planet. Space Sci. 18(6), 929-938, 1970.

Moe, K., Bowman, B. R. The effects of surface composition and treatment on drag coefficients of spherical satellites, AAS 2005-258. American Astronautical Society Publications Office, San Diego, CA , 2005.

Moe, K., DeBra, D. B., Van Patten, R. A., Moe, M. M., Oelker, G., Ruggera, Jr., M. B. Exospheric density measurements from the drag-free satellite Triad. J. Geophy Res. 81, 3753-3761, 1976

Moe, K., Moe, M. M. Deduction of in-track winds from satellite measurements of density and composition. Geophys. Res. Let. 19, 1343-1346, 1992.

Moe, K., Moe, M. M. Gas-surface interactions and satellite drag coefficients. Plan. Space Sci. 53, 793-801, 2005.

Moe, K., Moe, M. M. The high-latitude thermospheric mass-density anomaly: A historical review and a semi-empirical model. J. Atmos.Solar-Terr. Phys. 70, 794-802, DOI 10.1016/j.jastp.2007.10.007, 2008.

Moe, K., Moe, M. M. Operational models and drag-derived density trends in the thermosphere. Space Weather 9, S00E10, doi:10.1029/2010SW000650, 2011.

Moe, M. M., Moe, K., The roles of kinetic theory and gas-surface interactions in measurements of upper-atmospheric density. Planet. Space Sci. 17(5), 917-922, 1969.

Moe, M.M., Wallace, S. D., Moe, K. Recommended drag coefficients for aeronomic satellites, in The Upper Mesosphere and Lower Thermosphere, AGU Monograph 87, American Geophysical Union, Washington, 1995.

Moe, K., Moe, M. M., Wallace, S. D. Improved satellite drag coefficient calculations from orbital measurements of energy accommodation. J. Spacecraft Rockets 35, 266-272, 1998.

Moe, K., Moe, M. M., Rice, C., J. Simultaneous analysis of multi-instrument satellite measurements of atmospheric density. J. Spacecraft Rockets 41, 849-853, 2004.

Murr , L. E., Kinard, W. H., Effects of low Earth orbit, American Scientist, 81, 152-165, 1993.

Newell, P. T., Meng, C.-I. The cusp and the cleft/boundary layer…J. Geophys. Res. 93, 14545-14549, 1988.

Newton, G. P., Resolution of the difference between atmospheric density measurements.J. Geophys. Res. 74, 6409-6414, 1969.

Nier, A. O., Mass spectrometry of the neutral constituents of the atmosphere. Mass Spectroscopy 15, 67-81, 1967.

Nier, A. O., Measurement of thermospheric composition, Space Res. XII, Vol. 2, 881- 889, Akademie Verlag, Berlin, 1972.

Obayashi, T., Matuura, N. Theoretical model of F-region storms, in: Dyer, E. J. (Ed.) Proceedings of the Symposium on Solar-Terrestrial Physics, Washington, D. C., 1971.

Offermann, D., Grossmann, U. Neutral composition measurements with a helium-cooled ion source. Space Research XII, North-Holland, Amsterdam, 1972, pp. 665-668.

Olson, W. P. Corpuscular radiation as an upper atmospheric energy source, in Space Res. XII, b, Akademie-Verlag, Berlin, 1007-1013, 1972.

Olson, W. P., Moe, K. Influence of precipitating charged particles on the high-latitude thermosphere. J. Atmos. Terr. Phys. 36, 1715-1726, 1974.

Pardini, C., Personal communication, 2008.

Pardini, C., Anselmo, L., Moe, K., Moe, M. M., Drag and energy accommodation coefficients during sunspot maximum, Adv. Space Res., 45, 638-650, 2010.

Pardini C., Moe, K., Anselmo., L. Thermospheric model biases at sunspot maximum. Submitted to Advances in Space Research, 2011.

Pearson, J. A., The Low-G Accelerometer Calibration System, Aerospace Rep. no. TR-0074 (4260-10)-1, Vol. 1 and 2, The Aerospace Corp., El Segundo, CA, 1973.

Picone, J.M., Emmert, J.T., Lean, J. Thermospheric densities derived from spacecraft orbits – I. Accurate processing of two-line element sets, J. Geophys. Res. 110, A03301, doi:10.1029/2004JA010585, 2005.

Pilinksi, M. D., Argro, B., Palo, S. E. Drag coefficients of satellites with concave geometries: Comparing models and observations. J. Spacecraft Rockets 48, 312-325, 2011a, doi:10.2514/1.50915.

Pilinski, M. D., Moe, K., Argrow, B., Palo, S. E., Measuring absolute thermospheric densities and accommodation coefficients using paddlewheel satellites: Past findings, present uses, and future mission concepts, Advances in the Astronautical Sciences, in press, 2011b.

Puderbaugh, A. L., Dixon, Jr., G. L., Shroyer, L. E., Boyce, W. H., Shepperd, R. W. A local and global history of drag effects at Iridium mission altitude. AIAA 02-613, Am. Inst. of Aeronautics and Astronautics, Reston, VA, 2002.

Qian, L., Roble, R. G., Solomon, S. C., Kane, T. J. Calculated and observed climate change in the thermosphere, and a prediction for solar cycle 24. Geophys Res. Let. 33, L23705, doi:10.1029/2006GL027185, 2006.

Qian, L., Solomon, S. C., Kane, T. J. Seasonal variation of thermospheric density and composition. J. Geophys. Res. 114, A01312, doi:10.1029/2008JA013643, 2009.

Rees, M. H. Physics and Chemistry of the Upper Atmosphere. Cambridge University Press, Cambridge, 1990.

Reiter, G. S., Moe, K. Surface-particle-interaction measurements using paddlewheel satellites. Proc. 6th Intl. Symposium on Rarefied Gas Dynamics, Academic Press, N. Y., Vol. 2, 1543-1555, 1969.

Richards, P. G. Ion and neutral density variations during ionospheric storms…J. Geophys. Res.,(A11), 1361, doi: 10.1029/2002JA009278, 2002.

Riley, J. A., Giese, C. F. Interaction of atomic oxygen with various surfaces. J. Chem. Phys. 53, 146-152, 1970.

Rim, H.-J., Webb, C. E., Yoon, S., Schutz, B. E., Macro-model tuning experiment for ICESAT precision orbit determination, paper AAS 07-165. American Astronautical Society Publications Office, San Diego, CA , 2007.

Saltsburg, H., Smith, J. N., Jr., Rogers, M., (Eds.). Fundamentals of Gas-Surface Interactions. Academic Press, N. Y., 346-391, 406-414, and 448-521, 1967.

Sentman, L. H. Free molecule flow theory and its application to the determination of aerodynamic forces. Lockheed Missile and Space Company, LMSC-448514, Sunnyvale, CA, 1961a

Sentman, L. H. Comparison of the exact and approximate methods for predicting free-molecular aerodynamic coefficients. Amer. Rocket Soc. J. 31, 1576-1579, 1961b.

Shepherd, G. G., Thirkettle, E. W. Magnetospheric dayside cusp: A topside view of its 6300 A emission. Science 180, 737-739, 1973.

Soddy, F., Berry, A. J. Proc. Roy. Soc., A83, 258, 1910.

Solomon, S. C., Woods, T. N., Didkovsky, L. V., Emmert, j. T., Qian, L. Anomalously low solar euv irradiance and thermospheric density during solar minimum, Geophys. Res. Let. 37, L16103, doi:10.1029/2010GL044468, 2010.

Spencer, N. W., Taeusch, D. R., Carignan, G. R. Annls. Geophys. 22, 151-160, 1966.

Sutton, E. K. Normalized force coefficients for satellites with elongated shapes, J. Spacecraft Rockets 46, 112-116, 2009.

Stickney, R. E. and Hurlbut, F. C., in Rarefied Gas Dynamics, Third Symposium, Academic Press, N.Y., 1963.

Thomas, L. B. Accommodation of molecules on controlled surfaces. Rarefied Gas Dynamics, Proceedings of Twelfth Symposium, 1980.

Tobiska, W. K. Validating the solar EUV proxy, E10.7. J. Geophys. Res. 106, A12, 29969-29978, 2001.

Tobiska, W. K., Bouwer, S. D., Bowman, B. R. The development of new solar indices for use in thermospheric density modeling. J. Atmos. Solar-Terr. Phys. 70, 803-819, 2008.

Torr, D. G., Torr, M. R., Richards, P. G. Thermospheric airglow emissions: A comparison of measurements from Atlas-1 with theory. Geophys. Res. Let. 20, 519-522, 1993.

Trinks, H., von Zahn, U., Reber, C. A., Hedin, A. E., Spencer, N. W., Krankowsky, D., Lammerzahl, P., Kayser, D. C., Nier, A. O. Intercomparison of neutral composition Measurements… J. Geophys. Res. 82, 1261-1265, 1977.

Vokrouhlický, D., Farinella, P., Mignard, F. Solar radiation pressure perturbations for earth satellites, III. Global atmospheric phenomena and the albedo effect. Astronomy and Astrophysics, 290:324–334, 1994.

Vokrouhlický, D., Farinella, P., Mignard, F., Solar radiation pressure perturbations for earth satellites, IV. Effects of the earth's polar flattening on the shadow structure and the penumbra transitions. Astronomy and Astrophysics, 307:635–644, 1996.

Wolverton, R. W. Flight Performance Handbook for Orbital Operations, Wiley, N. Y. and London, 2-389 to 2-397, 1963.

Wood, B. J. The rate and mechanism of interaction of oxygen atoms and hydrogen atoms with silver and gold. J. Phys. Chem. 75, 2186-2193, 1971.

Ziebart, M. Generalized analytical solar radiation pressure modeling algorithm for spacecraft of complex shape, J. Spacecraft Rockets 41, 840, 2004.

Ziebart, M., Adhya, S., Sibthorpe, A., Edwards, S., and Cross, P. Combined radiation pressure and thermal modelling of complex satellites: Algorithms and on-orbit tests. Advances in Space Research 36(3):424–430, 2005.

Table 1. Estimated measurement uncertainties

Property	% Accuracy	References
Uncooled Mass Spectrometers:		Nier (1972)
Density	15-20	Trinks, et al. (1977)
Molecular nitrogen	25	Killeen, et al. (1989)
Molecular oxygen	15-20	
Atomic oxygen (from O_2)	15-20	
Helium	75	
Cooled Mass Spectrometers:		Offermann and Grossmann (1972)
All constituents	30	
Extinction (absorption):		Hinteregger and Hall (1969)
Density	25	
Composition	100	
Emission (far UV):		Rees (1990), Huffman (1992)
All constituents	20-100	Torr, et al. (1993), Majeed, et al. (1993), Budzien, et al., (1994)
Scale Height:		Moe (1970)
O / N_2	30	
Drag Density (C_d corrected):		Moe et al. (1995)
Smooth Spheres	10	Moe, et al. (1998)
Long cylinders	15	Bowman and Moe (2005)
		Pardini, et al. (2009)
		Doornbos, et al. (2009)

Table 2. Examples of model biases
Estimated percentages by which the J70MOD model densities are too high

Altitude (km)	Solar Minimum (%)	Solar Maximum (%)
150		4
200	7	6
250	10	8
300	13	9
350		10
400		12
500		12

Table 3. Examples of model biases
Percentage by which density models are too high at sunspot maximum
(percentage by which C_D is too low)

Altitude (km)	J70 MOD	JB2006
150	4	7
200	6	9
250	8	11
300	9	12
350	10	13
400	12	15
500	12	15

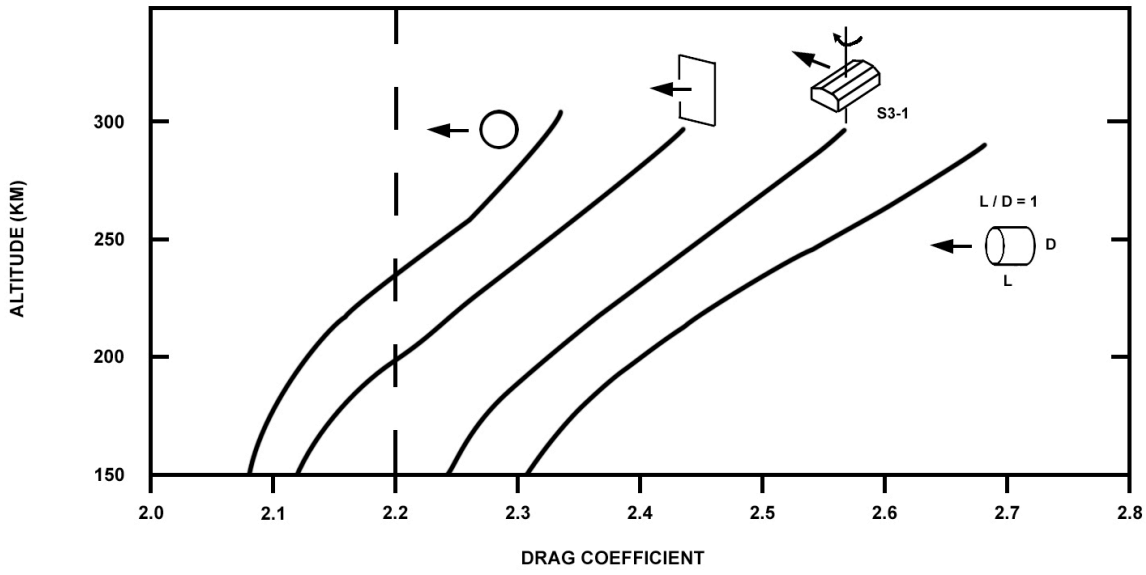

Figure 1. Drag coefficients of four compact satellite shapes versus altitude near sunspot minimum